Putrescine Activation of *Trypanosoma cruzi S*-Adenosylmethionine Decarboxylase†

Tracy Clyne, Lisa N. Kinch,‡ and Margaret A. Phillips*

Department of Pharmacology, The University of Texas Southwestern Medical Center at Dallas, 5323 Harry Hines Boulevard, Dallas, Texas 75390-9041

Received July 30, 2002; Revised Manuscript Received September 5, 2002

ABSTRACT: *S*-Adenosylmethionine decarboxylase (AdoMetDC) is a pyruvoyl-dependent enzyme that is processed from a single polypeptide into two subunits creating the cofactor. In the human enzyme, both the proenzyme processing reaction and enzyme activity are stimulated by the polyamine putrescine. The processing reaction of *Trypanosoma cruzi* AdoMetDC was studied in an *in vitro* translation system. The enzyme was fully processed in the absence of putrescine, and the rate of this reaction was not stimulated by addition of the polyamine. Residues in the putrescine binding site of the human enzyme were evaluated for their role in processing of the *T. cruzi* enzyme. The E15A, I80K/S178E, D174A, and E256A mutant *T. cruzi* enzymes were fully processed. In contrast, mutation of R13 to Leu (the equivalent residue in the human enzyme) abolished processing of the *T. cruzi* enzyme, demonstrating that Arg at position 13 is a major determinant for proenzyme processing in the parasite enzyme. This amino acid change is a key structural difference that is likely to be a factor in the finding that putrescine has no role in processing of the *T. cruzi* enzyme. In contrast, the activity of *T. cruzi* AdoMetDC is stimulated by putrescine. Equilibrium sedimentation experiments demonstrated that putrescine does not alter the oligomeric state of the enzyme. The putrescine binding constant for binding to the *T. cruzi* enzyme (K_d = 150 μM) was measured by a fluorescence assay and by ultrafiltration with a radiolabeled ligand. The mutant *T. cruzi* enzyme D174V no longer binds putrescine, and is not activated by the diamine. In contrast, mutation of E15, S178, E256, and I80 had no effect on putrescine binding. The k_{cat}/K_m values for E15A and E256A mutants were stimulated by putrescine to a smaller extent than the wild-type enzyme (2- and 4-fold vs 11-fold, respectively). These data suggest that the putrescine binding site on the *T. cruzi* enzyme contains only limited elements (D174) in common with the human enzyme and that the diamine plays different roles in the function of the mammalian and parasite enzymes.

S-Adenosylmethionine decarboxylase (AdoMetDC)[1] catalyzes the pyruvoyl-dependent decarboxylation of *S*-adenosylmethionine, a key step of polyamine biosynthesis. The product of the reaction provides aminopropyl groups for the formation of the polyamines spermidine and spermine, which are required for cell growth (*1*). The polyamine biosynthetic pathway is a proven drug target against African sleeping sickness caused by the parasite *Trypanosoma brucei*; inhibitors of ornithine decarboxylase are used clinically, and inhibitors of AdoMetDC have proven to be effective in animal models (*2*−*5*). A specific inhibitor of AdoMetDC reduces the infectivity of *Trypanosoma cruzi* parasites that cause Chagas disease (*6*), and knockout cell lines of the related parasite *Leishmania donovani* are putrescine auxotrophs (*7*). These data suggest that AdoMetDC may also be a target for rational drug development in these related parasites.

AdoMetDC belongs to a small class of enzymes that use a pyruvoyl cofactor for catalysis (*8*). The X-ray structure of the human enzyme has been determined in complex with several inhibitors (*9*−*11*). The pyruvoyl group promotes catalysis by forming a Schiff base with the amino group of the substrate, thus providing an electron sink to stabilize the carbanion that is generated upon decarboxylation. These enzymes are synthesized as a propeptide. The polypeptide is subsequently proteolyzed in an autocatalytic reaction into α and β subunits, generating the pyruvate prosthetic group at the amino terminus of the α subunit. The chemistry of the processing reaction was first demonstrated for histidine decarboxylase (*12*), and recent studies have provided insight into the mechanism of processing for AdoMetDC. In these studies, the ester intermediate formed in the processing reaction was trapped by mutation of H243 (*10*, *13*).

The mammalian AdoMetDC enzyme is regulated at many levels (*8*). Putrescine, which is the precursor to the higher polyamines, enhances the rate of formation of the pyruvoyl cofactor and stimulates enzyme activity. However, this

† This work was supported by grants (to M.A.P.) from the National Institutes of Health (R01 AI34432) and the Welch Foundation (I-1257) and by predoctoral training grants (to T.C. and L.N.K.) from the National Institutes of Health (T32 GM08203 and T32 GM08297). M.A.P. is a recipient of a Burroughs Wellcome Fund Scholar Award in Molecular Parasitology.

* To whom correspondence should be addressed. Telephone: (214) 648-3637. Fax: (214) 648-9961. E-mail: margaret.phillips@UTSouthwestern.edu.

‡ Present address: Howard Hughes Medical Institute and Department of Biochemistry, University of Texas Southwestern Medical Center, 5323 Harry Hines Blvd., Dallas, TX 75390-9050.

[1] Abbreviations: AdoMetDC, *S*-adenosylmethionine decarboxylase. Residues are numbered on the basis of the human sequence, and mutations are denoted by their single-amino acid code, e.g., Arg-13 to Leu substitution is L13R.

10.1021/bi026541d CCC: $22.00
Published on Web 10/12/2002

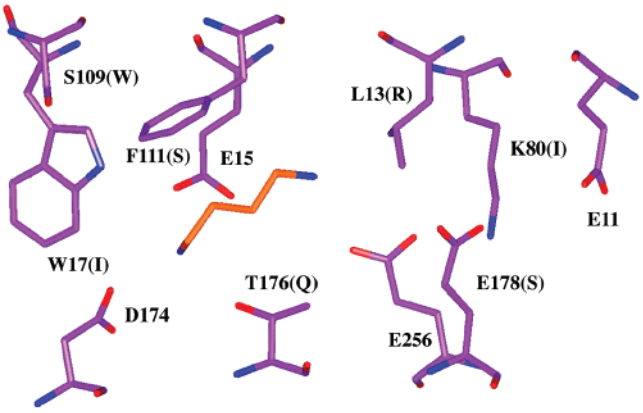

FIGURE 1: Putrescine binding site in human AdoMetDC. The X-ray structure of human AdoMetDC [PDB entry 1JL0 (*10*)] is displayed with the program Insight II (Accelyrs Inc., San Diego). Carbon atoms are displayed in purple (protein) or orange (putrescine), oxygens in red, and nitrogens in blue. The putrescine binding site is adjacent to the active site, which contains E11. S113 is not shown for clarity, but it is positioned near L13. Residues are numbered and labeled according to the human sequence. For positions with variable amino acids in the *T. cruzi* enzyme, the *T. cruzi* sequence is displayed in parentheses.

regulation is species specific. The effect of putrescine on proenzyme processing has been studied in only a limited number of cases; putrescine had no effect on the processing of the enzymes from *Neurospora crassa* (*19*), or that from plants (*14*). Studies on the role of putrescine in stimulating enzyme activity are more numerous; putrescine enhances the activity of AdoMetDC from a number of eukaryotic enzymes [*T. brucei* (*15*), *T. cruzi* (*16*, *17*), *Saccharomyces cerevisiae* (*18*), *N. crassa* (*19*), *Acanthamoeba culbertsoni* (*20*), and *Onchocerca vulvulus* (*21*)]. However, the diamine has no effect on the activity of the plant or malarial enzymes (*14*, *22*). While putrescine enhances the activity of the *T. cruzi* AdoMetDC, the concentration of diamine required to fully activate the enzyme is significantly higher than that required to activate the mammalian enzyme (*16*, *17*). The effect of putrescine on the processing reaction of the *T. cruzi* enzyme has not been well characterized.

The structural basis for activation by putrescine has been studied in the human enzyme by X-ray crystallography and site-directed mutagenesis. The X-ray structure reveals a single putrescine bound within the β-sandwich protein core (*10*). Direct H-bonds are formed with E15, D174, and T176, and several other acidic residues form interactions through bound water molecules (E178 and E256; Figure 1). This binding site is adjacent to the active site, but too distant to allow putrescine to be directly involved in the chemistry of the reaction, suggesting an allosteric mechanism for its effects. Mutation of residues E11, K80, E174, E256, and E178 reduces the level of putrescine stimulation of the processing reaction (*23*), while mutation of E178, E256, and D174 also decreases the extent of putrescine stimulation of enzyme activity (*14*, *24*). Though several of the residues that have been identified to have a role in modulation of the human enzyme by putrescine are conserved across a diverse group of species, a number of others differ in the sequences from the protozoan parasites and from plants (Table 1). These divergences in the sequence of the putrescine binding site suggest that differences in the mechanism of putrescine activation of processing and enzyme activity will be observed.

Table 1: *T. cruzi* and Plant Amino Acid Substitutions Identified in the Putrescine Binding Site of Human AdoMetDC[a]

residue number	human	*T. cruzi*	plant
13	Leu	Arg	Arg
15	Glu	Glu	Glu
80	Lys	Ile	Lys
111	Phe	Ser	Lys/Arg
113	Ser	Met	Thr
174	Asp	Asp	Met/Val/Ile
176	Thr	Gln	Thr
178	Glu	Ser	Glu
256	Glu	Glu	Glu

[a] Amino acid residues are numbered on the basis of the human sequence. A multiple-sequence alignment of eukaryotic AdoMetDC enzymes (accession number PF01536) obtained from the PFAM database (*35*) guided our assignment of structurally equivalent residues for the plant and parasite enzymes. This alignment was compared to the X-ray structure of human AdoMetDC complexed to putrescine to determine the identity of the residues at these positions (Figure 1).

In this paper, we explore the role of putrescine in activation of the polypeptide processing reaction and on enzyme activity in AdoMetDC from *T. cruzi*. Processing of the *T. cruzi* enzyme is not facilitated by putrescine. A key amino acid substitution of a residue that is in the putrescine binding site of the human enzyme (L13 in the human enzyme is replaced with R13 in the *T. cruzi* enzyme) is essential for processing of the *T. cruzi* enzyme; the R13L mutant of *T. cruzi* AdoMetDC is unable to process. These data suggest that the amino acid substitution at this position is an important structural change that removes a role for putrescine in the processing reaction of the parasite enzyme. Putrescine activation of enzyme activity in the *T. cruzi* enzyme was also studied. Putrescine does not influence the oligomeric state of the enzyme, nor does it form a Schiff base with the catalytic pyruvoyl moiety. An assessment of putrescine binding to the *T. cruzi* enzyme by fluorescence demonstrates that it is bound more weakly to the *T. cruzi* enzyme than to the human enzyme. Of the residues that are important for putrescine activation of human AdoMetDC, only D174 plays a role in putrescine binding and stimulation of the *T. cruzi* enzyme. These studies demonstrate that putrescine plays different roles in the function of AdoMetDC from different organisms, and that it is likely to have a different binding mode in the parasite enzyme.

EXPERIMENTAL PROCEDURES

Materials

S-Adenosyl[*carboxy*-^{14}C]methionine (56 mCi/mmol) and [^{14}C]putrescine (114 mCi/mmol) were purchased from Amersham Pharmacia Biotech (Arlington Heights, IL). Ni^{2+}–agarose was purchased from Qiagen Inc. (Chatsworth, CA). Restriction enzymes were purchased from New England Biolabs (Beverly, MA) or Boehringer Mannheim (Indianapolis, IN). All other reagents were purchased from Sigma (St. Louis, MO).

Expression and Purification of T. cruzi AdoMetDC

AdoMetDC was expressed and purified as a His-tagged fusion using the gene cloned from *T. cruzi* in a T7 bacterial

expression construct as previously described (*17*). *Escherichia coli* BL21/DE3 cells containing this construct were grown in a New Brunswick BioFlo 3000 fermentor, and the recombinant enzyme was purified using Ni^{2+}−agarose column chromatography and anion exchange column chromatography. All purification buffers lacked putrescine. The purified protein was quantitated using the extinction coefficient previously determined for the native enzyme (46.5 mM^{-1} cm^{-1}).

Human AdoMetDC Cloning and Expression

The human AdoMetDC gene was amplified from human prostate QUICK-CloneTM cDNA (Clontech Labs, Inc.) using the PCR primers 5′-TGGGCCCATGGAAGCTGCACATTTTTTCGAAGGGACCG-3′ and 5′-ACGCTGTCGACTCAACTCTGCTGTTGTTGCTGCTTCTTAGC-3′. The PCR product was cloned into the *Nco*I and *Sal*I sites of the expression plasmid ODC29 (*25*) to generate the human expression plasmid pSam18. The human insert was sequenced, and the protein was expressed and purified as previously described for the *T. cruzi* enzyme (*17*). The resulting clone contains a single mutation (R33C) that we found fortuitously increases the expression levels without affecting function. This residue is not fully conserved across different species and is located on the surface of the enzyme distant from the active site and the putative putrescine binding site. The human enzyme expresses to high levels, producing 200 mg of purified enzyme from a 6 L preparation. The purified recombinant protein is correctly processed into a 31 kDa α subunit and a 7.5 kDa β subunit. Gel filtration of the recombinant human enzyme predicts a molecular mass of 73 kDa in the presence of putrescine, which is consistent with a dimer of $\alpha\beta$ subunits.

Site-Directed Mutagenesis of T. cruzi AdoMetDC

To create the various mutant AdoMetDC enzymes, PCR-based site-directed mutagenesis using the Stratagene QuikChange kit was performed using the *T. cruzi* AdoMetDC expression plasmid as a template. The constructs were verified by sequencing.

In Vitro Translation and Proenzyme Processing

Wild-type and mutant AdoMetDC proteins were synthesized *in vitro* using the T7-coupled transcription/translation kit (Promega) with [^{35}S]methionine to label the protein as described previously (*23*). Each reaction included 0.2 μg of plasmid, 9.4 pmol of [^{35}S]methionine (total volume of 0.05 mL), and 2 mM putrescine when indicated. The transcription/translation reaction mixture was incubated at 30 °C for 30 min, at which time cycloheximide was added to a final concentration of 0.2 mM to stop translation. The reaction mixtures were incubated at 30 °C to allow proenzyme processing to continue, and aliquots were removed at 0, 15, 30, and 60 min for analysis by a 15% SDS−PAGE. The gel was prepared for audioradiography by fixing in destain (5% MeOH and 7% acetic acid) for 30 min, washing with H_2O, soaking in sodium salicylate for 5 min, and washing with H_2O. The gel was then dried and exposed to Reflection NEF-496 film (Du Pont) overnight. Relative amounts of processed versus unprocessed protein were quantified using NIH image (National Institutes of Health, Bethesda, MD).

Analytical Ultracentrifugation

Equilibrium sedimentation data for the *T. cruzi* AdoMetDC enzyme were collected in a Beckman XLI analytical ultracentrifuge. Samples were analyzed at 20 °C in buffer [50 mM Hepes (pH 8.0), 100 mM NaCl, and 0.5 mM β-mercaptoethanol] with or without 10 mM putrescine. Three enzyme concentrations (initial absorbancies of 0.2, 0.4, and 0.5, respectively) were loaded into a six-sector equilibrium centerpiece and equilibrated at three rotor speeds (11 000, 13 000, and 15 000 rpm). Absorption data were collected through quartz window assemblies at 280 nm, using a radial step size of 0.001 cm, and recorded as the average of 15 measurements at each radial position once samples were judged to have reached equilibrium. The nine data sets for each enzyme were analyzed with Beckman XL-A.XL-I Data Analysis Software version 4.0 and globally fit to the appropriate model using a monomer molecular weight of 43 974 and a molar extinction coefficient of 46 500 cm^{-1} M^{-1}. The baseline values were allowed to float, and υ-bar (0.731 mL/g) and ρ (1.00 g/mL) were fixed during the fit to values determined using the program SEDNTERP (*26*). The goodness of fit was determined by examination of the residuals and minimization of the variance. The data were best fit to a monomer−dimer equilibrium in all cases.

Cyanoborohydride Reduction of the Substrate and Activator

To determine the extent of Schiff base formation on the enzyme, sodium cyanoborohydride ($NaCNBH_3$) was used as a reducing agent (*27*). The reaction mixtures contained wild-type AdoMetDC (430 μM) and either $^{14}CO_2$-AdoMet (56 mCi/mol, 44 μM) or [1,4-^{14}C]putrescine (114 mCi/mmol, 44 μM) in buffer [200 mM HEPES (pH 7.5)] in a final volume of 0.02 mL. $NaCNBH_3$ was added to a final concentration of 5 mM, and the reaction mixtures were incubated for 20 min at 37 °C and then stored at 4 °C overnight. The protein was precipitated by adding 7.5% TCA. The amount of radioactivity was measured in both the precipitate and the supernatant to determine the extent of Schiff base formation. The precipitated protein was run on SDS−PAGE and stained with Coomassie blue. The extent of radioactive incorporation was visualized after using the EN^{3}HANCE autoradiography enhancer as recommended by the manufacturer (NEN Research Products) with a 6 day exposure.

Putrescine Binding Assays

Putrescine Binding As Assessed by Tryptophan Fluorescence. Mixtures of AdoMetDC (1−5 μM) in buffer [50 mM HEPES (pH 8.0), 50 mM NaCl, and 2.5 mM DTT] were titrated with increasing amounts of either putrescine or NaCl in a total of 1 mL. A difference emission spectrum in the presence and absence of putrescine was generated using a fluorometer (Photon Technology International) to find the wavelength with the largest change upon excitation at 280 nm. The emission spectrum was collected in 1 or 2 nm intervals from 300 to 400 nm in the absence or presence of 10 mM putrescine. The fluorescence intensity in the presence of saturating putrescine (F) was then subtracted from the fluorescence intensity in the absence of putrescine (F_0).

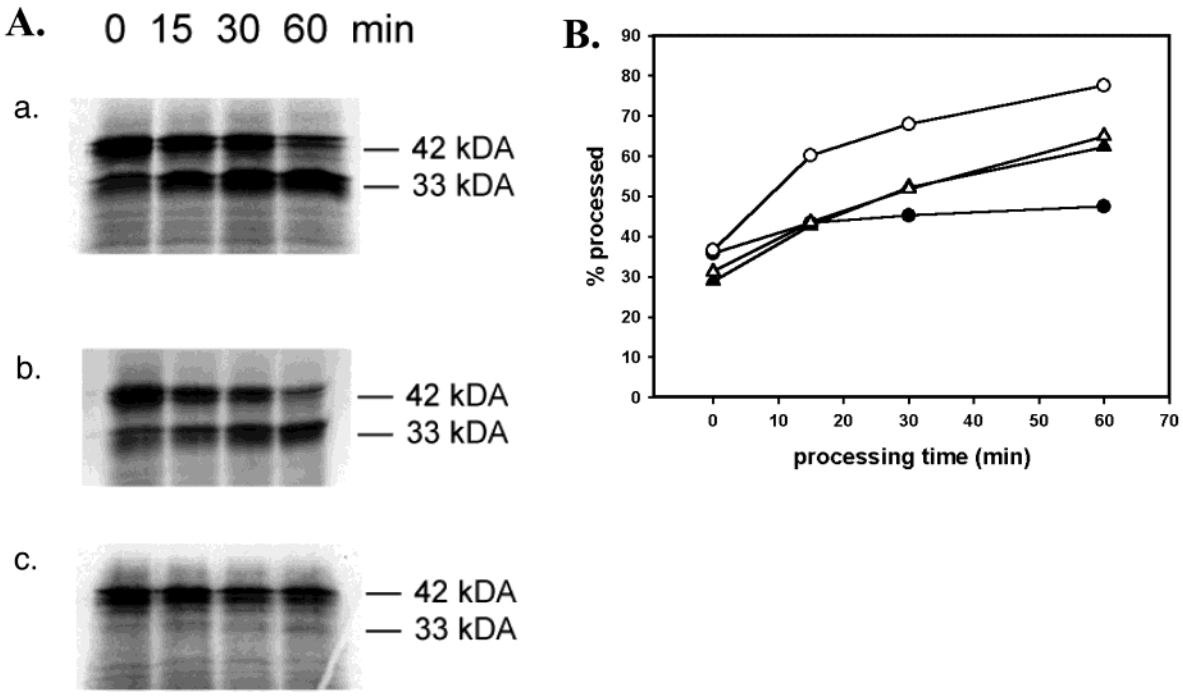

FIGURE 2: Proenzyme processing of *T. cruzi* and human AdoMetDC. (A) *T. cruzi* AdoMetDC was expressed in an *in vitro* rabbit reticulocyte system in the presence of [^{35}S]Met. Reactions were stopped by the addition of cycloheximide, and the mixtures were incubated for 0, 15, 30, and 60 min before analysis. The protein was subjected to SDS−PAGE and visualized by autoradiography: (a) wild-type enzyme in the absence of putrescine, (b) wild-type enzyme in the presence of 2 mM putrescine, and (c) R13L *T. cruzi* AdoMetDC in the presence of 2 mM putrescine. (B) Percent of the processed enzyme plotted vs incubation time: human AdoMetDC (circles) and *T. cruzi* AdoMetDC (triangles), and without putrescine (filled symbols) and with putrescine (empty symbols).

Titrations of putrescine were then performed by adding increasing amounts of putrescine (0.02−10 mM) and measuring the emission at 340 nm at 1 s intervals for 20 s. The measurements were repeated, and the 40 fluorescent intensity points were averaged to obtain a single intensity for the putrescine concentration. Under these conditions, very little photobleaching of the enzyme was detected. As a control, increasing amounts of NaCl were added to an equivalent mixture in parallel. The average of the putrescine intensity (F) was subtracted from the average of the NaCl intensity (F_0) and then plotted against putrescine concentration. The K_d for putrescine was then determined by fitting the data to eq 1

$$F - F_0 = \frac{[L]F_{max}}{K_D + [L]} \quad (1)$$

where L represents the putrescine ligand.

Binding of [^{14}C]Putrescine. Equilibrium product binding to *T. cruzi* or human AdoMetDC was assessed using ultrafiltration to separate free ligand (*28*). Various concentrations of [1,4-^{14}C]putrescine (10−320 μM for *T. cruzi* or 1.5−80 μM for human AdoMetDC) were mixed with AdoMetDC (80−100 μM for *T. cruzi* or 9.4 μM for human AdoMetDC) in buffer [50 mM HEPES (pH 8.0), 50 mM NaCl, and 2 mM DTT]. Mixtures were incubated at 4 °C overnight. A microcon-10 microconcentrator (Amicon) was used to separate a small portion of free ligand (5−6 μL) from the total volume (0.1 mL) by spinning at 14000*g* for 7 s. The concentrations of free ligand ([L_f]) and total ligand were determined by measuring the amount of radioactivity in an aliquot of sample (2 μL). The bound ligand ([L_B]) concentration was calculated by subtracting free from total, and the data were fitted to eq 2.

$$[L_B] = \frac{n[E][L_f]}{K_D + [L_f]} \quad (2)$$

Steady-State Kinetic Analysis

Steady-state kinetic analysis of AdoMetDC was performed as previously described (*17*). Reactions were carried out in buffer [200 mM HEPES (pH 8.0), 100 mM NaCl, and 5 mM DTT] at various AdoMet (0.01−10 mM) and putrescine concentrations (0−45 mM). Reaction mixtures were incubated at 37 °C for 5, 10, and 20 min at various enzyme concentrations (0.5−6.5 μM) to ensure a linear rate with time. Data were fitted to the Michaelis−Menten equation to determine the rate constants K_m and k_{cat}.

RESULTS

Effects of Putrescine on Autocatalytic Processing of T. cruzi AdoMetDC. To test if proenzyme processing of *T. cruzi* AdoMetDC is stimulated by putrescine, the enzyme was expressed in an *in vitro* rabbit reticulocyte system in the presence and absence of putrescine. The processing reaction was monitored by SDS−PAGE analysis after addition of cycloheximide and incubation of the translation product for increasing amounts of time. The rate of processing of *T. cruzi* AdoMetDC was not affected by the addition of putrescine (2 mM) to the reaction mixture (Figure 2). In contrast, as reported previously (*23*), both the rate and extent of the processing reaction for the human enzyme were increased by the addition of putrescine.

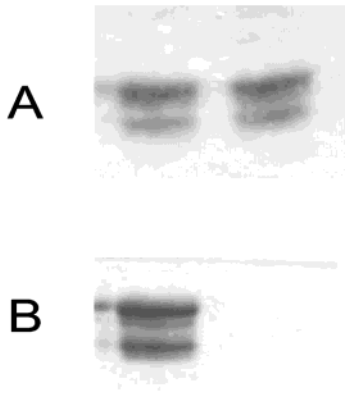

FIGURE 3: Analysis of Schiff base intermediates formed with *T. cruzi* AdoMetDC. [$^{14}CH_3$]AdoMet (lane 1) and [^{14}C]putrescine (lane 2) were incubated with *T. cruzi* AdoMetDC (0.43 mM) and reduced with sodium cyanoborohydride. Panel A shows a Coomassie blue-stained SDS gel (15%) of the AdoMetDC α subunit. Panel B shows a 6 day exposure of the same gel and represents the radioactive ligand covalently attached to the α subunit after reduction. The α subunit typically runs as two bands on SDS−PAGE (*17*).

The X-ray structure of human AdoMetDC bound to putrescine identifies the amino acid residues in the binding site (*10*). Several of these residues differ in the *T. cruzi* enzyme, suggesting that the roles and function of putrescine and its interacting residues may also differ. Notably, the *T. cruzi* enzyme contains a positive charge at position 13 (Figure 1 and Table 1), which is present in the protozoal (including the kinetoplastids and *Plasmodium* species) and plant enzymes. The equivalent residue in the human enzyme is L13, which is 3.4 Å from the bound putrescine residue. To test if the Arg in this position of the *T. cruzi* enzyme is able to substitute for the role of putrescine in the processing reaction, R13 in the *T. cruzi* enzyme was mutated to Leu. The R13L mutant enzyme is expressed as a proenzyme in the rabbit reticulocyte system, but it fails to process to the mature form after extended incubation in the presence or absence of putrescine (Figure 2). These data demonstrate that R13 is an essential residue for proenzyme processing in the *T. cruzi* enzyme, and they identify a fundamental difference in the structural requirements for proenzyme activation between the *T. cruzi* and human enzymes.

Analysis of Schiff Base Intermediates Formed with T. cruzi AdoMetDC by Trapping with Cyanoborohydride. The putrescine activator contains two free amino groups that could form a Schiff base with the pyruvate cofactor on the AdoMetDC enzyme. Therefore, putrescine could enhance the rate of Schiff base formation with AdoMetDC by allowing the chemistry to proceed through a gemdiamine intermediate instead of a carbinolamine intermediate. Pyridoxal phosphate (PLP)-dependent enzymes utilize this approach to accelerate Schiff base formation with the substrate through the formation of an internal aldimine between PLP and an active site Lys residue (*29*−*31*). To test this hypothesis, either radiolabeled putrescine or AdoMet was incubated with the *T. cruzi* AdoMetDC enzyme (0.43 mM) and the mixture was treated with sodium cyanoborohydride to reduce any Schiff base species that was formed. The protein samples were evaluated by SDS−PAGE and autoradiography. Radiolabeled AdoMet was readily incorporated onto the protein; however, no radioactive putrescine was detected in the protein band (Figure 3). The absence of any radioactivity suggests that the putrescine does not form a Schiff base with pyruvate.

Analysis of the Oligomeric State of T. cruzi AdoMetDC by Equilibrium Sedimentation. AdoMetDC is a homodimer of $\alpha\beta$ subunits. The X-ray structure of the human enzyme demonstrates that the active sites are contained within each enzyme monomer and that they are distant from the dimer interface, suggesting that the enzyme is not an obligate dimer (*9*). Therefore, an allosteric mechanism would be required for dimerization to influence the decarboxylation rate of the enzyme. To test the hypothesis that putrescine increases AdoMetDC activity by altering the dimeric state of the enzyme, purified recombinant *T. cruzi* AdoMetDC was analyzed by equilibrium sedimentation in a Beckman analytical ultracentrifuge in the presence and absence of putrescine (10 mM). For each analysis, nine data sets consisting of three different speeds and three different enzyme concentrations were utilized in a global fit of the data to various oligomeric models. In all cases, the data for *T. cruzi* AdoMetDC were best fit by a dimer−monomer equilibrium with a K_d of 15−30 μM in the absence or presence of putrescine (Figure 4). These data demonstrate that the dimer is not essential to the catalytic activity of the protein, as the enzyme is fully active at enzyme concentrations of <0.5 μM. Further, putrescine has no effect on the dimeric state of the *T. cruzi* enzyme.

Assessment of Putrescine Binding to T. cruzi AdoMetDC by Fluorescence and by Ultrafiltration. Intrinsic tryptophan fluorescence measurements provide a method of evaluating ligand interactions in cases where the environment of a Trp residue changes upon ligand binding (*32*). Therefore, the effect of putrescine on the intrinsic Trp fluorescence of the AdoMetDC enzyme was measured. Figure 5A illustrates the fluorescence emission spectrum of the *T. cruzi* AdoMetDC enzyme compared to that of free Trp in buffer. The emission maximum (λ_{max}) of the enzyme is shifted toward a wavelength (335 nm) lower than that of the free Trp (355 nm). Because the emission spectrum of Trp shifts to shorter wavelengths as the polarity of the solvent decreases (*33*), the measured fluorescence emission of the AdoMetDC enzyme is due to a buried Trp residue on the protein. The addition of putrescine (10 mM) to the enzyme yields a measurable decrease in emission intensity (Figure 5B,C), which is accompanied by a slight shift in the peak maximum toward a lower wavelength ($\lambda_{max} = 332$ nm). The wavelength showing the maximum difference in the presence of saturating putrescine (340 nm) was then used to further characterize the effects of putrescine concentration on fluorescence (Figure 5D). The data were fitted to eq 1 to determine the dissociation constant (K_d) for the putrescine ligand (150 ± 20 μM).

To provide additional support for the idea that the K_d determined from the fluorescence analysis represents ligand binding, equilibrium binding analysis of radioactive putrescine ([^{14}C]putrescine) to the *T. cruzi* AdoMetDC enzyme was performed by ultrafiltration (Figure 6). The dissociation constant measured by this method ($K_d = 180 \pm 100$ μM, $n = 1.6 \pm 1.1$) is similar to that determined from the fluorescence binding assay. These results validate the use of the fluorescence assay in assessing putrescine binding. Finally, the K_d measured for putrescine binding is significantly lower than the concentration of putrescine ($K_{m,put} =$

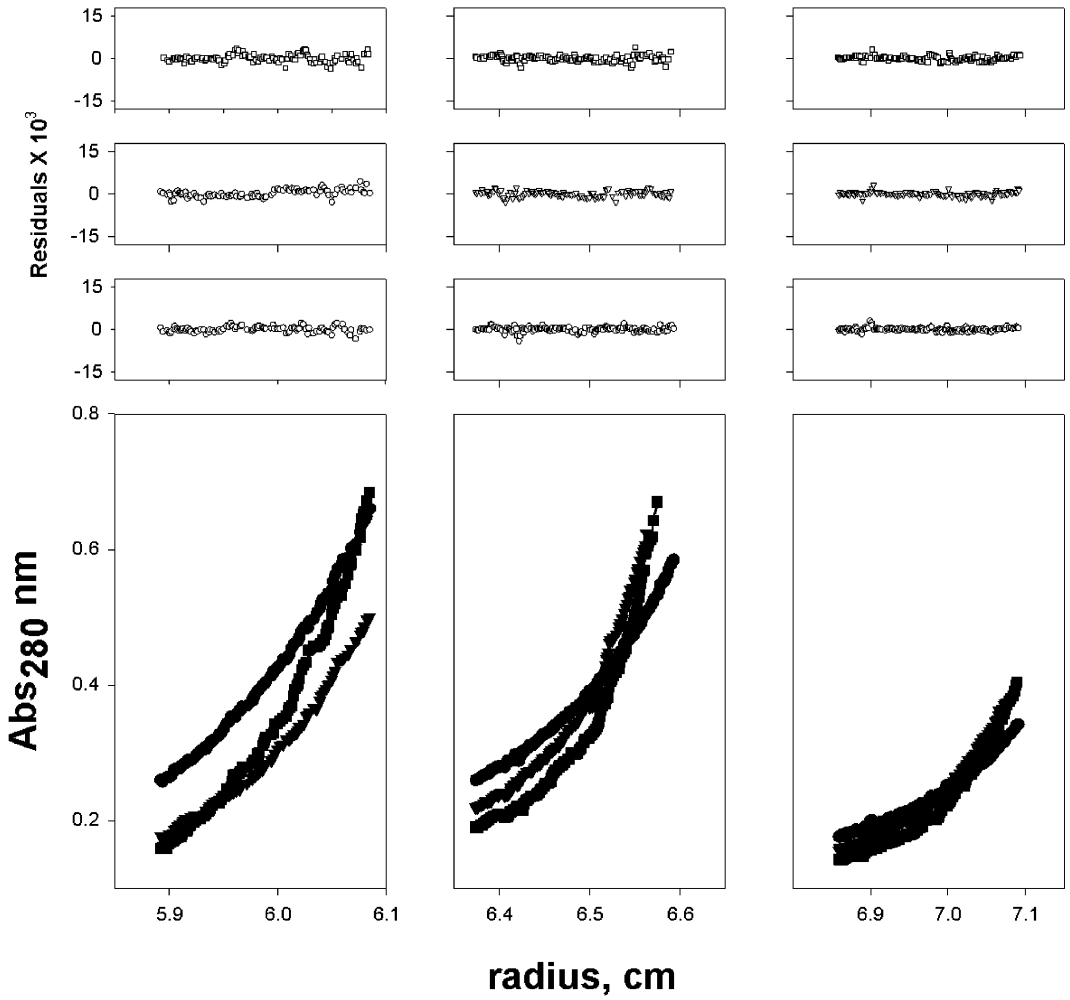

FIGURE 4: Sedimentation equilibrium analysis of *T. cruzi* AdoMetDC. Wild-type *T. cruzi* AdoMetDC was analyzed by sedimentation equilibrium in a Beckman XLI analytical ultracentrifuge in the presence and absence of 10 mM putrescine. A representative data set in the presence of putrescine is displayed. Dimerization constants (K_d) were determined by global analysis of nine data sets acquired at three speeds (11 000, 13 000, and 15 000 rpm) and three protein concentrations (4.3, 8.6, and 10.8 μM). For this data set, the fitted $K_d = 14$ μM, with a 95% confidence limit of 12−16 μM.

4.7 mM) required to fully activate the enzyme (Table 2), reflecting a complexity in the kinetic model of activation.

Putrescine Binding to Human AdoMetDC. Steady-state kinetic analysis of the human AdoMetDC enzyme at pH 8.0 in the presence of the saturating putrescine activator (2 mM) produces a K_m for AdoMet (70 ± 17 μM) and a k_{cat} (0.7 ± 0.07 s^{-1}) similar to those previously described (*24*). As previously reported, the overall rate of the human reaction is much faster than that of the parasite enzyme (*17*). Comparison of the apparent putrescine activation constants for human and *T. cruzi* AdoMetDC determined by kinetic analysis [for human, $K_{m.put} = 0.13$ mM (*34*); for *T. cruzi*, $K_{m.put} = 4.7$ mM (Table 1)] suggests that putrescine may bind tighter to the human AdoMetDC than to the parasite enzyme. However, kinetic analysis does not allow for the measurement of a true dissociation constant. Therefore, binding of putrescine to the human enzyme was also studied by fluorescence and by equilibrium binding to [^{14}C]putrescine. The human enzyme exhibits a smaller change in the fluorescence emission intensity in the presence of the putrescine activator than the *T. cruzi* AdoMetDC enzyme, and instead of a decrease in fluorescence being seen, an increase is observed (Figure 5E). The maximum fluorescence emission intensity difference occurred at 332 nm, and it varies with putrescine concentration. Titration of the fluorescence emission intensity at 332 nm was used to measure a binding isotherm for putrescine ($K_d = 5 \pm 3$ μM). The K_d determined by fluorescence is again similar to that measured by Scatchard analysis of equilibrium binding of the human AdoMetDC enzyme to [^{14}C]putrescine ($K_d = 6 \pm 1$ μM, $n = 1.5 \pm 0.1$), validating the fluorescence method for the human enzyme. The data demonstrate that the human enzyme binds putrescine with a higher affinity than the parasite enzyme; thus, the differences in putrescine concentration required to activate the two enzymes are also reflected in a difference in affinity. However, as with the *T. cruzi* enzyme, the K_d for putrescine is significantly lower than the $K_{m.put}$ (0.13 mM) reported for the human enzyme based on kinetic analysis (*34*). Thus, kinetic analysis of enzyme activation by putrescine does not provide direct information about binding affinity for putrescine in either the *T. cruzi* or human enzyme.

Site-Directed Mutagenesis of Putative Putrescine Binding Site Residues. A number of residues have been identified in the putrescine binding site of human AdoMetDC [E15, K80, D174, E178, and E256 (*10*); Figure 1], and several of these residues have been reported to be required for putrescine stimulation of activity [D174, E178, and E256 (*14*, *23*)]. Of

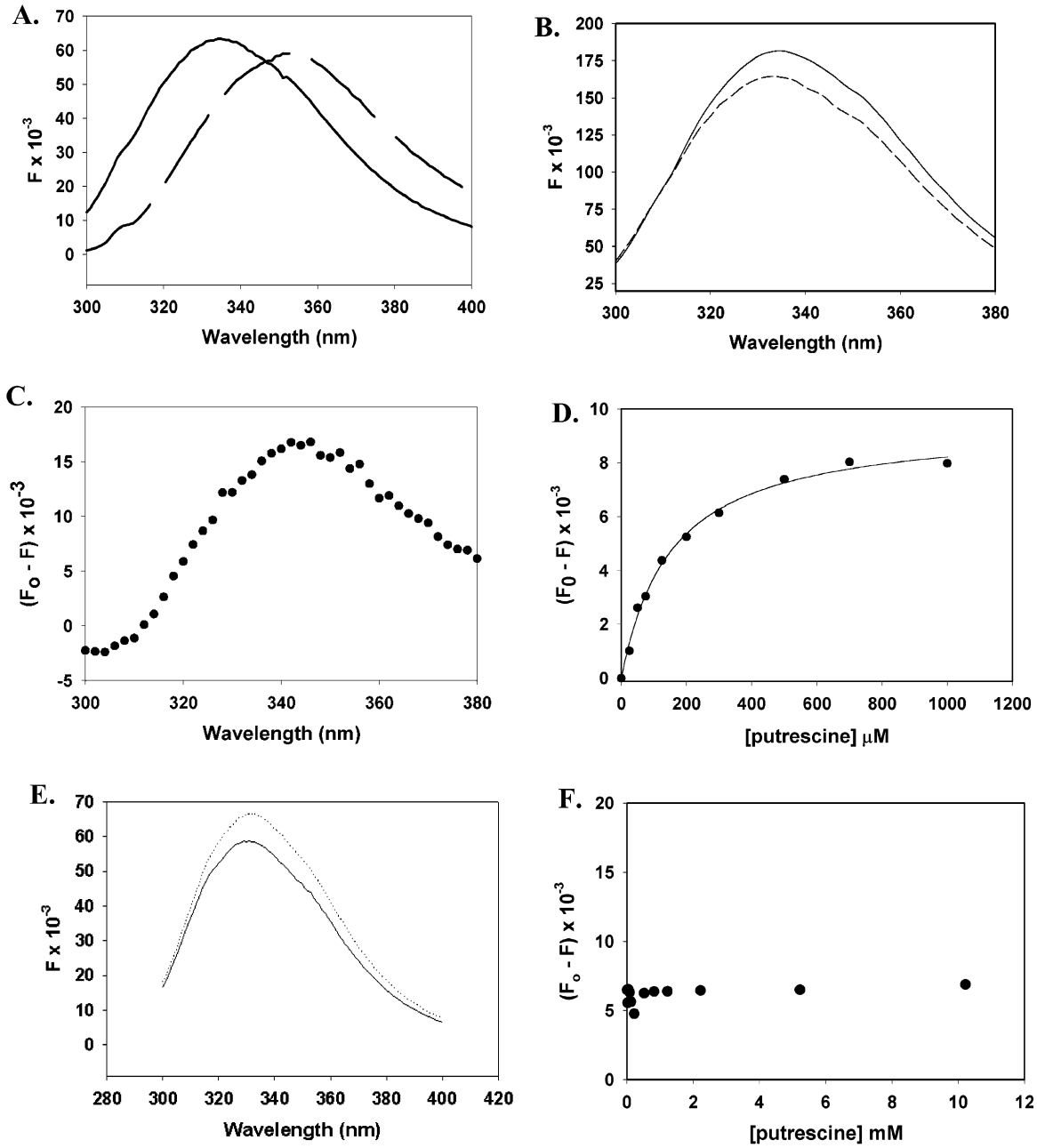

FIGURE 5: Analysis of putrescine binding to *T. cruzi* AdoMetDC by intrinsic fluorescence emission. Panel A shows the fluorescence (*F*) emission spectrum of *T. cruzi* AdoMetDC (—) and tryptophan (···) after excitation at 280 nm. The λ_{max} for the enzyme is 335 nm, while the λ_{max} for the tryptophan is 355 nm. Panel B shows the fluorescence emission change of *T. cruzi* AdoMetDC (—) upon addition of 10 mM putrescine (···). Panel C shows the difference spectrum of the intensity in the presence of putrescine (*F*) subtracted from the intensity in the presence of the same concentration of NaCl as a control (F_0). The wavelength with the maximum change is 340 nm. Panel D shows the dependence of $F_0 - F$ at 340 nm on the putrescine concentration. The data were fitted to eq 1 to yield a K_d of 150 ± 20 μM. Errors are the standard error of the fit. In panel E, the fluorescence (*F*) emission change of human AdoMetDC (—) upon addition of 1 mM putrescine (···) is shown. In panel F is shown the analysis of putrescine binding to *T. cruzi* AdoMetDC D174V. The fluorescence emission difference ($F_0 - F$) is displayed at 340 nm for the titration from 0 to 10 mM putrescine.

these residues, E15, E256, and D174 are conserved in the *T. cruzi* enzyme while E178 and K80 are not (Table 1). To determine the roles of these residues in the putrescine activation of the *T.cruzi* enzyme, these residues were mutated. The conserved residues E15 and E256 were replaced with Ala, and D174 was mutated to Val, the residue found in this position in plants (Table 1). E178 and K80 form a salt bridge in the human enzyme. These residues are neutral residues in the *T. cruzi* enzyme (I80 and S178). The double mutant I80K/S178E was constructed in the *T. cruzi* enzyme to create an enzyme that contained the same residues as the human enzyme in these positions. All four mutant enzymes (E15A, E256A, D174V, and I80K/S178E) were expressed normally and were processed to the mature form of the enzyme.

The effects of the mutations on putrescine binding and activation were characterized for each. E256A and I80K/S178E bind putrescine with an affinity similar to that of the wild-type enzyme, as measured by the fluorescence binding assay, while E15A binds with a 10-fold higher affinity (Table 2). I80K/S178E is activated by putrescine to the same extent as wild-type *T. cruzi* AdoMetDC (Table 2). However, E15A

Table 2: Summary of Putrescine Binding and Kinetic Analysis of Wild-Type and Mutant *T. cruzi* AdoMetDC[a]

		0 mM		45 mM			
putrescine enzyme	K_d^{Put}(Fl) (μM)	$K_{m.AdoMet}$ (mM)	k_{cat} (s^{-1})	$K_{m.AdoMet}^{Put}$ (mM)	k_{cat}^{Put} (s^{-1})	$K_{m.put}$ (mM)	k_{cat}/K_m (Put)/k_{cat}/K_m (no Put)
wild type	150 ± 10	0.66 ± 0.170	0.018 ± 0.002	0.28 ± 0.06	0.089 ± 0.007	4.7 ± 2.2	11
E15A	8 ± 4	0.96 ± 0.12	0.033 ± 0.002	0.81 ± 0.16	0.047 ± 0.005	7.9 ± 4.5	2
E256A	120 ± 10	2.7 ± 0.9	0.026 ± 0.007	2.0 ± 0.08	0.079 ± 0.002	2.0 ± 0.6	4
I80K/S178E	220 ± 80	4.0 ± 0.5	0.069 ± 0.008	1.0 ± 0.08	0.21 ± 0.009	9.0 ± 2.4	12
D174V	nd	0.73 ± 0.05	0.029 ± 0.001	2.0 ± 0.4	0.064 ± 0.009	nd	0.8

[a] K_d^{Put}(Fl) is the binding constant measured for putrescine by fluorescence as described in the legend of Figure 5. $K_{m.AdoMet}^{Put}$ and k_{cat}^{Put} are the steady-state parameters for AdoMet in the presence of 45 mM putrescine, and $K_{m.put}$ is the apparent Michaelis constant for putrescine collected at 0.3 mM AdoMet. nd, not detected. Errors are the standard error of the fit.

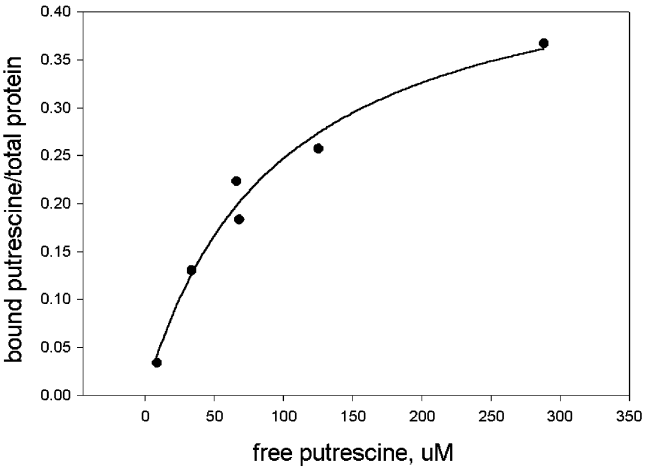

FIGURE 6: Scatchard analysis of radiolabeled putrescine binding. Equilibrium binding analysis of [^{14}C]putrescine with *T. cruzi* AdoMetDC was performed. The free ligand was separated by ultrafiltration. Data were fitted to eq 2 to determine a K_d of 94 ± 19 μM ($n = 0.5$) for this data set, where the errors are the standard error of the fit. The experiment was repeated three independent times, and the average parameters were determined ($K_d = 180 \pm 100$ μM, $n = 1.6 \pm 1.1$), where the error is the standard deviation of the mean.

and E256A were activated to a lesser extent than the wild-type enzyme; the k_{cat}/K_m increased by 2- and 4-fold for E15A and E256A, respectively, in comparison to 11-fold for the wild-type enzyme (Table 2). Thus, while these mutations do not disrupt putrescine binding, these residues do play some role in the mechanism of activation.

In contrast to these results, the fluorescence emission spectrum of the D174V mutant enzyme does not change as putrescine is titrated into the enzyme mixture over a broad concentration range of 0.02−10 mM putrescine (Figure 5F). Further, the D174V mutant is not activated by putrescine; the k_{cat}/K_m is unchanged in the presence of 45 mM putrescine (Table 2). These results demonstrate that the D174V mutant *T. cruzi* enzyme no longer binds putrescine, consistent with a role for D174 in forming a direct interaction with the positive charge of the putrescine. Thus, D174 is the one residue that plays a common role in putrescine binding between the mammalian and parasitic enzymes.

DISCUSSION

The role of putrescine in AdoMetDC processing and enzyme activity differs among the enzymes from different species. For the human enzyme, putrescine stimulates both processing and enzyme activity, while for the plant enzymes, putrescine plays no role in either process (*8*, *14*, *18*, *34*). While putrescine stimulates the activity of the *T. cruzi* enzyme, the data presented in this paper demonstrate that it has no role in proenzyme processing. Analysis of the amino acid sequences of the AdoMetDC enzymes from these various species provides clues about the involvement of different residues in the binding and activation process, therefore shedding light upon the physical basis of these responses. The residues making up the central core of the putrescine binding site of the human AdoMetDC enzyme contain several significant differences among enzymes from different species (Figure 1 and Table 1). Our data suggest that the substitution of an Arg residue for Leu at position 13 eliminates a role for putrescine in the proenzyme processing reaction of the *T. cruzi* enzyme, while the residue at position 174 determines if putrescine stimulates enzyme activity.

The residue at position 13 is Leu in the human enzyme and Arg in the *T. cruzi* and plant enzymes. This residue is within 3.4 Å of the putrescine binding site in the human AdoMetDC structure (*10*). Mutation of R13 to Leu in the *T. cruzi* enzyme renders the enzyme unable to process to the mature form, in either the presence or absence of putrescine. These data suggest that the presence of the positive charge at this position may mimic the positive charge of the putrescine molecule. Thus, this amino acid change is a key structural difference in the parasitic and plant enzymes that may underlie the finding that putrescine no longer plays a role in the proenzyme activation process. The requirement for putrescine in the processing reaction for the human enzyme is not however as strict as the requirement for R13 in the *T. cruzi* enzyme. The human enzyme is processed in the absence of putrescine, just at a slower rate (*14*). In addition, the processing of the *N. crassa* enzyme, which also has a Leu at position 13, is not stimulated by putrescine (*19*). Thus, R13 in the *T. cruzi* enzyme is likely to have additional functional roles in the processing reaction beyond the role of putrescine in the human enzyme, and additional structural differences between the enzymes may also be required to fully manifest these functions.

Insight into the mechanism by which putrescine stimulates enzyme activity in the *T. cruzi* enzyme can also be obtained by comparative analysis. D174 is conserved in the human and *T. cruzi* enzymes but is substituted with a Val in the plant enzymes (Table 1). The *T. cruzi* mutant enzyme D174V no loner binds putrescine, nor is it activated by putrescine. A similar result was reported for the activation of the mutant human enzyme D174V, though direct analysis of putrescine binding was not undertaken (*14*). Thus, the plant enzymes that contain Val at position 174 and Arg at position 13 would

not be expected to bind putrescine, consistent with the observation that neither processing nor enzyme activity is affected by putrescine. The enzyme from *Plasmodium falciparum* also lacks D174, and consistent with this structural change, the activity of this enzyme is not activated by putrescine (*22*).

The fact that putrescine cannot substitute for the absence of the positive charge in the R13L mutant processing reaction suggests that the diamine does not have the same binding mode on the parasite enzyme as observed for the human enzyme. Inspection of the putrescine binding site in the human structure provides additional support for this interpretation (Figure 1). The positive charge on R13 would be expected to have an unfavorable electrostatic interaction with putrescine if it were bound in the same site as observed for the human enzyme. In addition, the presence of the larger side chains of R13, Q176, and M113 in the binding site would also provide a likely steric block to ligand binding at this site. The mutagenesis data on the *T. cruzi* enzyme are consistent with this hypothesis. Mutation of E15 and E256, which are conserved in the putrescine binding site between human and *T. cruzi* AdoMetDC, had no effect on putrescine binding in the *T. cruzi* enzyme. The ion pair of E178 and K80 found in human AdoMetDC is replaced with Ser and Ile in the parasite enzymes. Mutation of these residues in the human enzyme results in an impaired ability of the enzyme to be activated by putrescine (*23*, *24*). In contrast, mutation of the *T. cruzi* residues to the ion pair found in the human enzyme had virtually no effect on putrescine binding or activation. Collectively, the lack of an influence of these residues on putrescine binding and activity suggests that the bound putrescine on the *T. cruzi* enzyme has been displaced from the position that is observed for the human enzyme and that it binds in a site that is at most only partially overlapping.

Although the exact position of the putrescine binding site in *T. cruzi* AdoMetDC awaits structure determination, clues to its position can be inferred from the comparative analysis of mutations described in this paper. D174 is the one common residue that appears to be involved in putrescine binding for both the *T. cruzi* and human enzymes. This residue is the most solvent-exposed of the interacting residues observed in the human enzyme structure. The more interior amino acid residues (E15, E256, K80, and E178) do not play a role in putrescine binding to the parasite enzyme, suggesting the binding site may be located closer to the surface. Further, the 10-fold decrease in putrescine affinity for the parasite enzyme suggests weaker interactions in the binding site that may stem from a more exposed location.

Finally, the observed fluorescence changes upon putrescine binding (Figure 5) suggest that the two enzymes exhibit a different environment surrounding the emitting Trp residue or residues. As a number of different Trp residues exist in both the human and *T. cruzi* enzymes, identification of the residues involved in the fluorescence change is difficult. However, both enzymes contain Trp residues (*T. cruzi* W109 and human W17) in the proximity of the common putrescine binding determinant D174. The carboxylate oxygen of D174 is 4.8 Å from the indole nitrogen of W17, while the side chain of position 109 is 2 Å further from both D174 and Nϵ1 of putrescine than is position 17 (Figure 1). These data are also consistent with a more exterior binding site for putrescine in the *T. cruzi* enzyme. Finally, the substitution of W17 with Ile, and F111 with Ser in the *T. cruzi* enzyme, could provide space for the putrescine binding site to be accommodated in this location.

We have used the differences in the activation of the human and parasite AdoMetDC enzymes to elucidate features of the putrescine binding site on the *T. cruzi* enzyme. Our data suggest that positions 13 and 174 are key determinants in the activation of processing and enzyme activity by putrescine. The parasite enzyme does not require putrescine to activate the processing reaction but instead Arg-13 is a major structural determinant required in the processing reaciton. D174 plays a role in binding putrescine in both the human and *T. cruzi* enzymes; however, the putrescine binding site is likely to only be partially overlapping between the two structures.

REFERENCES

1. Tabor, C. W., and Tabor, H. (1984) Polyamines, *Annu. Rev. Biochem. 53*, 749−790.
2. Wang, C. C. (1995) Molecular mechanisms and therapeutic approaches to the treatment of African Trypanosomiasis, *Annu. Rev. Pharmacol. Toxicol. 35*, 93−127.
3. Bacchi, C. J., Brun, R., Croft, S. L., Alicea, K., and Buhler, Y. (1996) In vivo trypanocidal activities of new S-adenosylmethionine decarboxylase inhibitors, *Antimicrob. Agents Chemother. 40*, 1448−1453.
4. Bacchi, C. J., Nathan, H. C., Yarlett, N., Goldberg, B., McCann, P. P., Bitonti, A. J., and Sjoerdsma, A. (1992) Cure of murine *Trypanosoma brucei rhodesiense* infections with an S-adenosylmethionine decarboxylase inhibitor, *Antimicrob. Agents Chemother. 36*, 2736−2740.
5. Tekwani, B. L., Bacchi, C. J., Secrist, J. A., and Pegg, A. E. (1992) Irreversible inhibition of S-adenosylmethionine decarboxylase of *Trypanosoma brucei brucei* by S-adenosylmethionine analogs, *Biochem. Pharmacol. 44*, 905−911.
6. Yakubu, M. A., Majumder, S., and Kierszenbaum, F. (1993) Inhibition of S-adenosyl-L-methionine (adomet) decarboxylase by the decarboxylated adomet analogue 5′-{[(Z)-4-amino-2-butenyl]-methylamino}-5′-deoxyadenosine (MDL73811) decreases the capacities of *Trypanosoma cruzi* to infect and multiply within a mammalian host cell, *J. Parasitol. 79*, 525−532.
7. Roberts, S. C., Scott, J., Gasteier, J. E., Jiang, Y., Brooks, B., Jarim, A., Carter, N. S., Heby, O., and Ullman, B. (2002) S-Adenosylmethionine decarboxylase from *Leishmania donovani*: molecular, genetic and biochemical characterization of null mutants and overproducers, *J. Biol. Chem. 277*, 5902−5909.
8. Pegg, A. E., Xiong, H., Feith, D. J., and Shantz, L. M. (1998) S-Adenosylmethionine decarboxylase: structure, function and regulation by polyamines, *Biochem. Soc. Trans. 26*, 580−586.
9. Ekstrom, J. L., Mathews, I. I., Stanley, B. A., Pegg, A. E., and Ealick, S. E. (1999) The crystal structure of human S-adenosylmethionine decarboxylase at 2.25 Å resolution reveals a novel fold, *Structure 7*, 583−595.
10. Ekstrom, J. L., Tolbert, W. D., Xiong, H., Pegg, A. E., and Ealick, S. E. (2001) Structure of a human S-adenosylmethionine decarboxylase self-processing ester intermediate and mechanism of putrescine stimulation of processing as revealed by the H243A mutant, *Biochemistry 40*, 9495−9504.
11. Tolbert, W. D., Ekstrom, J. L., Mathews, I. I., Secrist, J. A., III, Kappor, P., Pegg, A. E., and Ealick, S. E. (2001) The structural basis for substrate specificity and inhibition of human S-adenosylmethionine decarboxylase, *Biochemistry 40*, 9484−9494.
12. van Poelje, P. D., and Snell, E. E. (1990) Pyruvoyl-dependent enzymes, *Annu. Rev. Biochem. 59*, 29−59.
13. Xiong, H., and Pegg, A. E. (1999) Mechanistic studies of the processing of human S-adenosylmethionine decarboxylase proenzyme, *J. Biol. Chem. 274*, 35059−35066.

14. Xiong, H., Stanley, B. A., Tekwani, B. L., and Pegg, A. E. (1997) Processing of mammalian and plant S-adenosylmethionine decarboxylase proenzymes, *J. Biol. Chem. 272*, 28342−28348.
15. Tekwani, B. L., Bacchi, C. J., and Pegg, A. E. (1992) Putrescine activated S-adenosylmethionine decarboxylase from *Trypanosoma brucei brucei*, *Mol. Cell. Biochem. 117*, 53−61.
16. Persson, K., Aslund, L., Grahn, B., Hanke, J., and Heby, O. (1998) *Trypanosoma cruzi* has not last its S-adenosylmethionine decarboxylase: characterization of the gene and the encoded enzyme, *Biochem. J. 333*, 527−537.
17. Kinch, L. N., Scott, J., Ullman, B., and Phillips, M. A. (1999) S-Adenosylmethionine from *Trypanosoma cruzi*: cloning, expression and kinetic characterization of the recombinant enzyme, *Mol. Biochem. Parasitol. 101*, 1−11.
18. Poso, H., Hannonen, P., Himberg, J., and Janne, J. (1976) Adenosylmethionine decarboxylase from various organisms: relation of the putrescine activation of the enzyme to the ability of the organism to synthesize spermine, *Biochem. Biophys. Res. Commun. 68*, 227−234.
19. Hoyt, M. A., Williams-Abbott, L. J., Pitkin, J. W., and Davis, R. H. (2000) Cloning and expression of the S-adenosylmethionine decarboyxlase gene of *Neurospora crassa* and processing of its product, *Mol. Gen. Genet. 263*, 664−673.
20. Gupta, S., Shukla, O. P., and Walter, R. D. (1987) Putrescine-activated S-adeonsylmethionine decarboxylase from *Acanthamoeba culbertsoni*, *Mol. Biochem. Parasitol. 23*, 247−252.
21. Da'dara, A. A., Mett, H., and Walter, R. D. (1998) MGBG analogues as potent inhibitors of S-adenosylmethionine decarboxylase from *Onchocerca volvulus*, *Mol. Biochem. Parasitol. 97*, 13−19.
22. Wrenger, C., Luersen, K., Krause, T., Muller, S., and Walter, R. D. (2001) The *Plasmodium falciparum* bifunctional ornithine decarboxylase, S-adenosylmethionine decarboxylase, enables a well balanced polyamine synthesis without domain-domain interaction, *J. Biol. Chem. 276*, 29651−29656.
23. Stanley, B. A., and Pegg, A. E. (1991) Amino acid residues necessary for putrescine stimulation of human S-adenosylmethionine decarboxylase proenzyme processing and catalytic activity, *J. Biol. Chem. 266*, 18502−18506.
24. Stanley, B. A., and Pegg, A. E. (1994) Expression of mammalian S-adenosylmethionine decarboxylase in *E. coli*, *J. Biol. Chem. 269*, 7901−7907.
25. Osterman, A. L., Grishin, N. V., Kinch, L. N., and Phillips, M. A. (1994) Formation of functional cross-species heterodimers of ornithine decarboxylase, *Biochemistry 33*, 13662−13667.
26. Laue, T. M., Shah, B., Ridgeway, T. M., and Pelletier, S. L. (1992) in *Analytical Ultracentrifugation in Biochemistry and Polymer Science* (Harding, S., Rowe, A., and Horton, J., Eds.) pp 90−125, Royal Society of Chemistry, Cambridge, U.K.
27. Borch, R. F., Bernstein, M. D., and Durst, H. D. (1971) The cyabohydridoborate anion as a selective reducing agent, *J. Am. Chem. Soc. 93*, 2896−2904.
28. Sophianopoulos, J. A., Durham, S. J., Sophianopoulos, A. J., Ragsdale, H. L., and Cropper, W. P. (1978) Ultrafiltration is theoretically equivalent to equilibrium dialysis but much simpler to carry out, *Arch. Biochem. Biophys. 187*, 132−137.
29. Toney, M. D., and Kirsch, J. F. (1989) Direct Bronsted analysis of the restoration of activity to a mutant enzyme by exogenous amines, *Science 243*, 1485−1488.
30. Toney, M. D., and Kirsch, J. F. (1993) Lysine 258 in aspartate aminotransferase: enforcer of the Circe effect for amino acid substrates and general-base catalyst for the 1,3-prototropic shift, *Biochemistry 32*, 1471−1479.
31. Osterman, A. L., Brooks, H. B., Jackson, L., Abbott, J. J., and Phillips, M. A. (1999) Lys-69 plays a key role in catalysis by *T. brucei* ornithine decarboxylase through acceleration of the substrate binding, decarboxylation and product release steps, *Biochemistry 38*, 11814−11826.
32. Lakowicz, J. R (1983) *Principles of fluorescence spectroscopy*, Plenum Press, New York.
33. Freifelder, D. (1982) *Physical Biochemistry: applications to biochemistry and molecular biology*, W. H. Freeman and Co., San Francisco.
34. Zappia, V., Carteni-Farina, M., and Della Pietra, G. (1972) S-Adenosylmethionine decarboxylase from human prostate, *Biochem. J. 129*, 703−709.
35. Bateman, A., Birney, E., Durbin, R., Eddy, S. R., Finn, R. D., and Sonnhammer, E. L. (1999) Pfam 3.1: 1313 multiple alignments and profile HMMs match the majority of proteins, *Nucleic Acids Res. 27*, 260−262.

BI026541D